2007

Simulation of the Oxygen Reduction Reaction at an RDE in 0.5 M H_2SO_4 Including an Adsorption Mechanism

Qingbo Dong

Shriram Santhanagopalan

Ralph E. White
University of South Carolina - Columbia, white@cec.sc.edu

Publication Info

Published in *Journal of the Electrochemical Society*, Volume 154, Issue 9, 2007, pages A888-A899.

Dong, Q., Santhanagopalan, S., & White, R.E. (2007). Simulation of the Oxygen Reduction Reaction at an RDE in 0.5 M H_2SO_4 including an Adsorption Mechanism. *Journal of the Electrochemical Society*, *154*(9): A888-A899.
Publisher's Version: http://dx.doi.org/10.1149/1.2756994

Journal of The Electrochemical Society, **154** (9) A888-A899 (2007)
0013-4651/2007/154(9)/A888/12/$20.00 © The Electrochemical Society

Simulation of the Oxygen Reduction Reaction at an RDE in 0.5 M H_2SO_4 Including an Adsorption Mechanism

Q. Dong,* S. Santhanagopalan,* and R. E. White,z**

Department of Chemical Engineering, University of South Carolina, Columbia, South Carolina 29201, USA

Oxygen reduction on the surface of a rotating disk electrode (RDE) in 0.5 M H_2SO_4 is simulated by including mass transfer, adsorption, and charge transfer. A generalized model for the adsorption and reaction of several species is introduced. The oxygen reduction reaction is simulated as a limiting case where oxygen is the only species adsorbed, and oxygen reduction is the only reaction that takes place on the surface of the electrode. The model is based on the Nernst–Planck equations for mass transfer and the Butler–Volmer equation for electrochemical kinetics. The simulated polarization curves capture the change in the Tafel slopes, which are observed experimentally but cannot be explained by the normal four-electron-transfer mechanism. The adsorption model is compared with the four-electron-transfer model by fitting experimental data to both models using a nonlinear parameter estimation technique. The effects of changes in some important kinetic parameters are demonstrated.
 [DOI: 10.1149/1.2756994]

Manuscript received February 15, 2007; revised manuscript received May 22, 2007. Available electronically July 30, 2007.

The oxygen reduction reaction (ORR) has been studied by using a rotating disk electrode (RDE) in acidic electrolytes such as sulfuric, perchloric, hydrochloric, and organic acid solutions.[1-4] Several reaction pathways have been proposed for the ORR based on the RDE experimental data, of which the four-electron pathway is primarily used to characterize the behavior of this reaction at a platinum electrode or a glassy carbon electrode coated with platinum-based catalyst.[5,6] The overall ORR is given by

$$O_2 + 4H^+ + 4e^- \rightleftharpoons 2H_2O \quad [1]$$

where a mechanism that consists of four separate single-electron-transfer steps is implicitly assumed.

A linear Tafel plot is expected for this four-electron reaction mechanism when the potential is lower than the standard electrode potential of 1.229 V vs the standard hydrogen electrode (SHE). Note that all the potentials mentioned in this work are with respect to the SHE. The potential region of 1.0–0.6 V is where the polymer electrolyte membrane fuel cell (PEMFC) is operated practically. Important kinetic information such as the exchange current density and the transfer coefficient can be extracted by studying this voltage window for the ORR occurring at metal electrodes or carbon-supported platinum nanoparticle catalyst-coated electrodes.

Transitions in the Tafel slopes for the ORR are observed when experimental data is analyzed.[2-4,7-11] The Tafel slope is just about doubled in the higher current density (HCD) region (the potential region below about 0.8 V) compared to the lower current density (LCD) region (the potential region above 0.8 V). Table I presents a collection of examples from the literature which present changing Tafel slopes. When the temperature is around 298 K, the Tafel slope in the LCD region is around 60 mV/dec, which is close to $2.303RT/F$, whereas this value is about 120 mV/dec or $2 \times 2.303RT/F$ in the HCD region. The double Tafel slope phenomenon is observed at smooth surfaces such as electrodes made of polycrystalline Pt, Pt (111), Pt(100), or Pt alloy, etc., and at inert electrodes coated with nanosized carbon-supported Pt catalyst powder.[3] Various explanations have been suggested to explain the change in the Tafel slope,[12-17] and one of them is the oxygen adsorption mechanism,[14,16] which relates the change in the Tafel slope to the change in the applied potential. The adsorption of oxygen on the platinum surface is further complicated by the presence of other competing species and intermediates.[18,19] The adsorption of the anion HSO_4^- can compete with the molecular oxygen adsorption for the Pt site.[19] Reversible dissolution of water at the surface of the electrode can lead to PtOH formation in the potential region of 0.6–1.0 V vs SHE, and this process may interfere with the electrochemical reactions occurring at the surface of the electrode.[18]

In this work, a generalized model is presented for the adsorption of multiple species $R_{l,\mathrm{sur}}$. Each adsorbing species is assumed to be transported to the surface of the electrode and become adsorbed to the electrode surface to form $R_{l,\mathrm{ads}}$

$$R_{l,\mathrm{sur}} \rightleftharpoons R_{l,\mathrm{ads}} \quad [2]$$

where the subscripts sur and ads represent the species in the solution phase adjacent to the surface of the electrode and the species adsorbed on the electrode surface, respectively. The adsorbed species subsequently participates in a charge-transfer reaction together with other species P_i, which are involved in the reaction on the electrode directly without undergoing an adsorption step

$$R_{l,\mathrm{ads}} + \sum_i s_{\mathrm{i},j} P_i^{z_i} \rightleftharpoons n_j e^- \quad [3]$$

For example, the oxygen reduction mechanism is modeled using an intermediate step involving oxygen adsorption, during which the reactant oxygen is transferred to the solution phase adjacent to the electrode surface; then the oxygen reaches the electrode surface via an adsorption step, and it is assumed that only the adsorbed oxygen on the electrode can proceed to the charge-transfer reaction as shown below[5]

$$O_{2,\mathrm{sur}} \rightleftharpoons O_{2,\mathrm{ads}} \quad [4]$$

$$O_{2,\mathrm{ads}} + 4H^+ + 4e^- \rightleftharpoons 2H_2O \quad [5]$$

Models for Reactions 1-5 are presented below, with a detailed derivation of the kinetic equation for the adsorption mechanism. The models are compared by simulating the polarization curves for both the models and regression of transport and kinetic parameters for the ORR in 0.5 M H_2SO_4 solution at an RDE. The equations used for representing mass transfer are based on the Nernst–Planck equation, and the kinetic equations used for the boundary conditions are based on the Butler–Volmer equation. These equations were derived in detail for the RDE system by White et al.[20-22] The effect of oxygen adsorption is included in the kinetic equation for the adsorption mechanism. The models presented here are coded in the Fortran language and solved with a subroutine named general nonlinear equation solver.[23,24] The commercial software Comsol Multiphysics is also used to carry out the same calculations (excluding the regression part) for comparison. The simulation and regression results support the adsorption mechanism by showing a better fit to the experimental data[3] and a good prediction of the change in the Tafel slopes. The effects of important kinetic parameters such as the exchange current densities and the transfer coefficients in both models are studied.

* Electrochemical Society Student Member.
** Electrochemical Society Fellow.
z E-mail: white@engr.sc.edu

Table I. Literature showing double Tafel slopes for the ORR.

Catalyst/electrode	Tafel slopes LCD/HCD (mV/dec)	Other conditions
Pt(100) smooth surface[7]	65/120	0.05 M H_2SO_4 solution, 900 rpm, 50 mV/s, room temperature 1 atm O_2
Pt(110) smooth surface[7]	80/120	0.05 M H_2SO_4 solution, 900 rpm, 50 mV/s, room temperature 1 atm O_2
Pt(111) smooth surface[8]	61–66/118–162	1 M H_2SO_4 mixed with 0, 0.5, or 1 M K_2SO_4, 2000 rpm, 10 mV/s, 298.15 K, 1 atm O_2
Pt(100) smooth surface[8]	61–64/162–165	1 M H_2SO_4 mixed with 0, 0.5, or 1 M K_2SO_4, 2000 rpm, 10 mV/s 298.15 K, 1 atm O_2
Pt polycrystalline, smooth surface[8]	67–69/120–163	1 M H_2SO_4 mixed with 0, 0.5, or 1 M K_2SO_4, 2000 rpm, 10 mV/s 298.15 K, 1 atm O_2
Pt(100), Pt(111), smooth surface[9]	60/120	0.05 M H_2SO_4 solution, 900 rpm, 50 mV/s, 298 K, 313 K, 333 K, 1 atm O_2
Pt polycrystalline, Pt_3Ni-sputtered, Pt_3Co-sputtered, or Pt_3Co-annealed, smooth surface[2]	74–86/105–113	0.1 M $HClO_4$ solution, 1600 rpm, 20 mV/s, 293 K, 1 atm O_2
20% Pt/Vuclan XC72 carbon coated on carbon glass surface[3]	58–63/115–123	Catalyst loading: 14 $\mu g/cm^2$ 0.5 M H_2SO_4 solution, 1600 rpm, 5 mV/s 293 K, 303 K, 313 K, 333 K, 1 atm O_2
Pt plug, smooth surface[4]	59/112	1 M trifluromethane sulfuric acid (TFMSA) solution, 1000 rpm, 25 mV/s room temperature, 1 atm, O_2
Platinum microelectrode, 100 μm in diameter[10]	65–76/110–123	Nafion/water, vapor in a pressure vessel, no rotation, 1 mV/s, temperature 303–353 K, 5 atmO_2
Pt Pt_3Co, Pt_3Ni polycrystalline, Pt/C[11]	59–65/107–126	0.1 M $HClO_4$, 1600 rpm, 5 mV/s 293 K, 1 atm O_2
Pt, Pt_3Co, Pt_3Ni polycrystalline, Pt/C[11]	46–53/92–124	0.1 M $HClO_4$, 1600 rpm, 5 mV/s 333 K, 1 atm O_2

Model Equations

Mass-transfer equations.— The material balance for each species within the boundary layer near the surface of an RDE, in terms of dimensionless spatial coordinates (ξ), is of the following form[20-22,25]

$$\frac{D_i}{D_R}\frac{d^2c_i}{d\xi^2} + 3\xi^2\frac{dc_i}{d\xi} + \frac{z_iD_iF}{D_RRT}\left[c_i\frac{d^2\Phi}{d\xi^2} + \frac{dc_i}{d\xi}\frac{d\Phi}{d\xi}\right] = 0 \qquad [6]$$

where D_i is the diffusion coefficient of species i in cm^2/s, D_R is the diffusion coefficient of the limit reactant in cm^2/s, F is the Faraday constant with a value of 96,487 C/mol, R is the universal gas constant with a value of 8.3143 J/mol K, T is the absolute temperature in K, c_i is the concentration of species i in mol/cm^3, Φ is the potential in the solution within the diffusion layer in V, and the subscript i is the index of species. When Reaction 1 or Reactions 4 and 5 are under consideration, $i = 1$, 2, and 3 corresponding to O_2, H^+, and HSO_4^-, respectively. The homogeneous reaction term is omitted in Eq. 6. Also, the equations are solved in one spatial dimension. Following the estimation method in the book by Bard and Faulkner,[26] the thickness of the hydrodynamic boundary layer near the surface of the electrode is of the order of 1×10^{-3} cm in magnitude, at rotating speeds ranging from several hundred to several thousand revolutions per minute (rpm), whereas the radius of the disk is normally of the order of several millimeters. Hence the choice of a one-dimensional model is justified. The electroneutrality condition given by

$$\sum_i z_ic_i = 0 \qquad [7]$$

completes the set of equations needed to solve for the unknowns of concentration c_i and liquid potential Φ. All changes in the solution are assumed to be limited to a distance of $\xi < 2$ and hence the bulk conditions in the solution are assumed to prevail at $\xi \geqslant 2$. The boundary conditions in the bulk solution and at the electrode surface are given by[20-22,25]

$$c_i = c_{i,\infty}, \quad \Phi = \Phi_{RE} \quad \text{at } \xi = 2 \qquad [8]$$

and

$$\sum_{j=1}^{f}\frac{s_{i,j}i_j}{n_jF} = \frac{1}{\delta_D}\left[D_i\frac{dc_i}{d\xi} + z_ic_iF\frac{D_i}{RT}\frac{d\Phi}{d\xi}\right]_{\xi=0} \quad \text{at } \xi = 0 \qquad [9]$$

respectively, where $s_{i,j}$ is the stoichiometric coefficient of species i in reaction j, and n_j is the number of electrons transferred in reaction j when written using the reduction convention

$$\sum_i s_{i,j}M_{i,j}^{z_i} \rightarrow n_je^- \qquad [10]$$

Kinetic equation for the four-electron-transfer model.— The current densities (i_j) in Eq. 10 can be obtained from the Butler–Volmer expression[20-22,25]

$$i_j = i_{0,j}\left\{\exp\left(\frac{\alpha_{a,j}F}{RT}\eta_j\right) - \exp\left(-\frac{\alpha_{c,j}F}{RT}\eta_j\right)\right\} \qquad [11]$$

where

$$i_{0,j} = i_{0,j,ref}\prod_i\left(\frac{c_{i,0}}{c_{i,ref}}\right)^{\gamma_{i,j}} \qquad [12]$$

and the open-circuit potential of reaction j at the reference concentrations relative to a standard reference electrode of a given kind is expressed as[20-22,25]

$$U_{ref,j} = U_j^\theta - \frac{RT}{n_jF}\sum_i s_{i,j}\ln\left(\frac{c_{i,ref}}{\rho_0}\right) - U_{j,RE}^\theta + \frac{RT}{n_{j,RE}F}\sum_i s_{i,j,RE}\ln\left(\frac{c_{i,RE}}{\rho_0}\right) \qquad [13]$$

The overpotential for electrochemical reaction j, η_j in Eq. 11, is given as[20-22,25]

$$\eta_j = \Phi_{met} - \Phi_{RE} - (\Phi_0 - \Phi_{RE}) - U_{j,ref} + \frac{RT}{n_jF}\sum_i s_{i,j}\ln\left(\frac{c_{i,0}}{c_{i,ref}}\right) \qquad [14]$$

Also, $\gamma_{i,j}$ is assumed to be related to $s_{i,j}$ in the following way

$$\begin{cases} \gamma_{i,j} = p_{i,j} - \dfrac{\alpha_{a,j} s_{i,j}}{n_j} & \text{for anodic reactants} \\ \gamma_{i,j} = q_{i,j} + \dfrac{\alpha_{c,j} s_{i,j}}{n_j} & \text{for cathodic reactants} \end{cases} \quad [15]$$

and the reaction order constants $p_{i,j}$ and $q_{i,j}$ are related to $s_{i,j}$ by

$$\begin{cases} p_{i,j} = s_{i,j} \quad q_{i,j} = 0 & \text{if } s_{i,j} > 0 \\ p_{i,j} = 0 \quad q_{i,j} = -s_{i,j} & \text{if } s_{i,j} < 0 \end{cases} \quad [16]$$

The apparent transfer coefficients for a reaction sum up to the number of electrons transferred in that reaction, that is

$$\alpha_{a,j} + \alpha_{c,j} = n_j \quad [17]$$

Kinetic equation for the adsorption model.— The following assumptions are made in this derivation: there are no double-layer effects and the adsorption process is fast; the Langmuir isotherm is applicable; the adsorbed species at the electrode surface $R_{l,\text{ads}}$ occupies only one monolayer on the electrode surface and their concentration $c_{l,\text{ads}}$ is proportional to their corresponding fractional coverage (θ_l) at the electrode. Interactions among the adsorbed species are ignored for simplicity.

The following derivations are based on the adsorption mechanism that consists of an adsorption step and a charge-transfer step, as shown in reaction mechanisms 2 and 3. The adsorption step shown in Reaction 2 is a chemical reaction rather than an electrochemical reaction; however, in order to derive the kinetic expression for Reactions 2 and 3, it is convenient to express the rate equation in a form similar to that of an electrochemical reaction

$$i_{a,l} = -\left[k_l c_{R_l,0} \left(1 - \sum_{\substack{k=1 \\ k \neq l}}^{k=n_s} \theta_k - \theta_l \right) - k_l'' \theta_l \right] \quad [18]$$

where $i_{a,l}$ is the current density of the adsorption step at the electrode surface, and θ_l is the fraction of the electrode surface covered by the adsorbed species. The corresponding expression for Eq. 4 is

$$i_a = -\left[k c_{O_2,0} \left(1 - \sum_{\substack{k=1 \\ k \neq l}}^{k=n_s} \theta_k - \theta \right) - k'' \theta \right] \quad [19]$$

where i_a is the current density of the oxygen adsorption step at the electrode surface, θ is the fraction of the electrode surface covered by the adsorbed oxygen. The surface coverage (θ_l) in Eq. 18 is not an equilibrium value and hence cannot be obtained from the adsorption isotherms. In order to obtain an expression for the current density for the mechanism proposed in Reactions 2 and 3, it is necessary to eliminate the variable θ_l in the rate expressions for the individual steps as shown below.

The first step is to relate the rate of adsorption to the surface coverage at equilibrium. When the adsorption process is in equilibrium with the solution immediately adjacent to the electrode surface, the adsorption rate $i_{a,j}$ should be 0 because the rate of adsorption equals the rate of desorption, the net change in $c_{R_{j,\text{ads}}}$ is zero

$$0 = k_l c_{R_{l,0}} \left(1 - \sum_{\substack{k=1 \\ k \neq l}}^{k=n_s} \theta_{k,0} - \theta_{l,0} \right) - k_l'' \theta_{l,0} \quad [20]$$

where $\theta_{l,0}$ is the equilibrium fractional surface coverage of species l with respect to the concentration of the solution adjacent to the electrode surface. Solving for k_l'', we have

$$k_l'' = \frac{k_l c_{R_{l,0}} \left(1 - \sum_{\substack{k=1 \\ k \neq l}}^{k=n_s} \theta_{k,0} - \theta_{l,0} \right)}{\theta_{l,0}} \quad [21]$$

Substituting Eq. 21 into Eq. 18, we have

$$i_{a,l} = -\frac{k_l c_{R_l,0}}{\theta_{l,0}} \left[\theta_{l,0} \left(1 - \sum_{\substack{k=1 \\ k \neq l}}^{k=n_s} \theta_k \right) - \theta_l \left(1 - \sum_{\substack{k=1 \\ k \neq l}}^{k=n_s} \theta_{k,0} \right) \right] \quad [22]$$

If we define the rate constant for the adsorption reaction $(i'_{0,a,l})$ as follows

$$i'_{0,a,l} = -k_l c_{R_l,0} \quad [23]$$

we have

$$i_{a,l} = -\frac{i'_{0,a,l}}{\theta_{l,0}} \left[\theta_{l,0} \left(1 - \sum_{\substack{k=1 \\ k \neq l}}^{k=n_s} \theta_k \right) - \theta_l \left(1 - \sum_{\substack{k=1 \\ k \neq l}}^{k=n_s} \theta_{k,0} \right) \right] \quad [24]$$

For a charge-transfer step occurring at the surface of the electrode, as shown in Reaction 3, the current density can be expressed according to the Butler–Volmer equation. The adsorbed species is assumed to be reduced in the following derivation. However, the equations for the case of the adsorbed species being oxidized can be derived likewise. The Butler–Volmer equation for the charge-transfer step is of the following form

$$i_j = k_{a,j}'' \prod_i c_{i,0}^{p_{i,j}} \exp\left(\frac{\alpha_{a,j} F}{RT} V \right) - k'_{c,j} c_{R_{l,\text{ads}}} \prod_l c_{i,0}^{q_{i,j}} \exp\left(-\frac{\alpha_{c,j} F}{RT} V \right) \quad [25]$$

Because the adsorption reaction occurs only at the fraction of the electrode surface occupied by the active sites (θ_l) and the reverse reaction occurs only at the surface not covered by any adsorbed species, it is necessary to multiply the anodic part by the term $(1 - \sum_{\substack{k=1 \\ k \neq l}}^{k=n_s} \theta_k - \theta_l)$ and the cathodic part by θ_l in Eq. 25

$$i_j = k'_{a,j} \left(1 - \sum_{\substack{k=1 \\ k \neq l}}^{k=n_s} \theta_k - \theta_l \right) \prod_i c_{i,0}^{p_{i,j}} \exp\left(\frac{\alpha_{a,j} F}{RT} V \right) - k'_{c,j} \theta_l c_{R_{l,\text{ads}}} \prod_i c_{i,0}^{q_{i,j}} \exp\left(-\frac{\alpha_{c,j} F}{RT} V \right) \quad [26]$$

where $c_{i,0}$ is the concentration of anodic species i in the charge-transfer reaction in mol/cm^3, and $c_{R_l,\text{ads}}$ is the transient concentration of species l adsorbed on the electrode surface in mol/cm^3. The electrode potential V is given by[20-22,25]

$$V = \Phi_{\text{met}} - \Phi_0 \quad [27]$$

where both Φ_{met} and Φ_0 are measured with respect to the same reference electrode. The concentration of the adsorbed species $(c_{R_{l,\text{ads}}})$ can be expressed in terms of the fractional coverage (θ_l). Because it is assumed that the adsorbed species occupies a monolayer at the surface of the electrode, $c_{R_{l,\text{ads}}}$ is linearly related to the fractional coverage θ_l, i.e., $c_{R_{l,\text{ads}}}$ is related to the surface coverage (θ_l) by the following expression

$$c_{R_{l,\text{ads}}} = k_{l,\text{ads}} \theta_l \quad [28]$$

where $k_{l,\text{ads}}$ is a proportionally constant for the adsorption Reaction 1. The rate expression Eq. 26 can be rewritten in terms of the surface coverage (θ_l) as follows

$$i_j = k'_{a,j}\left(1 - \sum_{\substack{k=1\\k\neq l}}^{k=n_s} \theta_k - \theta_l\right)\exp\left(\frac{\alpha_{a,j}F}{RT}V\right) - k_{c,j}\theta_l^2 \exp\left(-\frac{\alpha_{c,j}F}{RT}V\right) \quad [29]$$

where $k'_{a,j}$ and $k_{c,j}$ are the new rate constants given by

$$k'_{a,j} = k'_{a,j}\prod_i c_{i,0}^{p_{i,j}} \quad [30]$$

$$k_{c,j} = k_{l,ads}k'_{c,j}\prod_i c_{i,0}^{q_{i,j}} \quad [31]$$

When the electrode is in equilibrium with the solution adjacent to the electrode surface, the current densities i_j should be 0 in Eq. 29

$$0 = k'_{a,j}\left(1 - \sum_{\substack{k=1\\k\neq l}}^{k=n_s} \theta_{k,0} - \theta_{l,0}\right)\exp\left(\frac{\alpha_{a,j}F}{RT}V_{0,j}\right) - k_{c,j}\theta_{l,0}^2 \exp\left(-\frac{\alpha_{c,j}F}{RT}V_{0,j}\right) \quad [32]$$

where $\theta_{l,0}$ is the surface coverage at equilibrium, and $V_{0,j}$ is the corresponding equilibrium electrode potential. Using Eq. 32 to define the equilibrium exchange current density $i'_{0,j}$ we have

$$i'_{0,j} = k'_{a,j}\left(1 - \sum_{\substack{k=1\\k\neq l}}^{k=n_s} \theta_{k,0} - \theta_{l,0}\right)\exp\left(\frac{\alpha_{a,j}F}{RT}V_{0,j}\right) = k_{c,j}\theta_{l,0}^2 \exp\left(-\frac{\alpha_{c,j}F}{RT}V_{0,j}\right) \quad [33]$$

Rewriting Eq. 32 in terms of $i'_{0,j}$, we have

$$i_j = i'_{0,j}\left[\frac{\left(1 - \sum_{\substack{k=1\\k\neq l}}^{k=n_s} \theta_k - \theta_l\right)}{\left(1 - \sum_{\substack{k=1\\k\neq l}}^{k=n_s} \theta_{k,0} - \theta_{l,0}\right)}\exp\left(\frac{\alpha_{a,j}F}{RT}\eta_j\right) - \left(\frac{\theta_l}{\theta_{l,0}}\right)^2 \exp\left(-\frac{\alpha_{c,j}F}{RT}\eta_j\right)\right] \quad [34]$$

where

$$\eta_j = V - V_{0,j} \quad [35]$$

$$i'_{0,j} = k'^{\alpha_{c,j}/n_j}_{a,j}k^{\alpha_{a,j}/n_j}_{c,j}(1 - \theta_{l,0})^{\alpha_{c,j}/n_j}\theta_{l,0}^{2\alpha_{a,j}/n_j}\prod_i c_{i,j}^{\gamma_{i,j}} \quad [36]$$

$$V_{0,j} = \frac{RT}{n_jF}\ln\left(\frac{k_{c,j}}{k'_{a,j}}\right) + \frac{RT}{n_jF}\ln\left(\frac{\theta_{l,0}^2\prod_i c_{i,j}^{s_{l,j}}}{\left(1 - \sum_{\substack{k=1\\k\neq l}}^{k=n_s} \theta_{k,0} - \theta_{l,0}\right)}\right) \quad [37]$$

Because we have assumed that there are no double-layer effects and that the adsorption step is fast, at steady state, the rate of the adsorption step should be the same as the charge-transfer step

$$i_j = i_{a,l} \quad [38]$$

This relationship can be used to eliminate the surface coverage (θ_l) between Eq. 24 and 33. The equilibrium surface coverage values ($\theta_{l,0}$) are usually obtained by holding a potential value for a particular time interval and integrating the charge passed in desorbing the adsorbed layer formed during a cathodic potential sweep.[18]

Limiting case of a single reaction.— The system of equations described above is complicated because of the simultaneous occurrence of several reactions at the electrode surface. However, when a simplifying assumption that the ORR is the only reaction occurring at the electrode surface can be made, a closed form solution for the surface coverage as well as the current at the surface of the electrode as functions of the electrode potential can be obtained. Such a limiting case analysis provides options to obtain kinetic parameters as described in the next section.

At the limiting case of ORR being the only reaction at the electrode surface, the following additional assumptions are made: surface the concentration of the solvent (water) is constant and the protons do not undergo an adsorption process. The surface coverage (θ) is assumed to be independent of the potential at the electrode surface. This assumption can readily be relaxed by introducing a function obtained from experimental data to relate the surface coverage to the surface potential; however, the derivation of such a function has been subject to criticism.[27,28] Equation 19 above is the rate expression for the adsorption step. However, because no other species is adsorbed on the electrode surface, we have

$$i_a = -[kc_{O_2,0}(1 - \theta) - k''\theta] \quad [39]$$

Because oxygen is the only species undergoing the adsorption process and Reaction 5 is the only charge-transfer reaction, the subscripts l and j are omitted. Equations 24 and 34 become

$$i_a = i'_{0,a}\frac{\theta - \theta_0}{\theta_0} \quad [40]$$

$$i = i'_0\left[\frac{1 - \theta}{1 - \theta_0}\exp\left(\frac{\alpha_aF}{RT}\eta\right) - \left(\frac{\theta}{\theta_0}\right)^2 \exp\left(-\frac{\alpha_cF}{RT}\eta\right)\right] \quad [41]$$

and Eq. 23, 28, and 35-37 become

$$i'_{0,a} = kc_{O_2,0} \quad [42]$$

$$c_{o_2,ads} = k_{ads}\theta \quad [43]$$

$$\eta = V - V'_0 \quad [44]$$

$$i'_0 = k'^{\alpha_c/4}_a k^{\alpha_a/4}_c c^{\alpha_a}_{H^+}(1 - \theta_0)^{\alpha_c/4}\theta_0^{\alpha_a/2} \quad [45]$$

$$V'_0 = \frac{RT}{4F}\ln\left(\frac{k_c}{k'_a}\right) + \frac{RT}{4F}\ln\left(\frac{\theta_0^2c_{H^+}^4}{1 - \theta_0}\right) \quad [46]$$

As indicated in Eq. 38, for the case of fast adsorption, the rate of the adsorption step should be the same as that of the charge-transfer step, and because in the limiting case there are no other reactions, the rates of adsorption and charge-transfer reaction are also the same as the total current density across the cell

$$i = i_a \quad [47]$$

This relationship can be used to eliminate the surface coverage (θ) in Eq. 40 and 41. The derivation of the relationship between the current density (i) to the cell potential (V) in terms of the equilibrium surface coverage (θ_0) and the concentration of oxygen at the surface of the electrode ($c_{O_2,0}$) is shown in the Appendix. A closed form solution and a limiting case are presented below. From Eq. 41, solving for θ we have

$$\theta = \theta_0 \sqrt{\frac{\exp\left(\frac{\alpha_a F}{RT}\eta\right) - \frac{i}{i_0'}}{\exp\left(-\frac{\alpha_c F}{RT}\eta\right)}} \quad [48]$$

Substituting Eq. 47 and the expression for θ (i.e., Eq. 48) into the rate expression for the adsorption step (i.e., Eq. 40) we have

$$i = i_{0,a}'\left(\sqrt{\frac{\exp\left(\frac{\alpha_a F}{RT}\eta\right) - \frac{i}{i_0'}}{\exp\left(-\frac{\alpha_c F}{RT}\eta\right)}} - 1 \right) \quad [49]$$

Solving for the current density across the cell (i) from the above equation gives

$$i = \frac{1}{2}\left(-2i_{0,a}' - X + \sqrt{X^2 + 4i_{0,a}'X + 4i_0'X\exp\left(\frac{\alpha_a F}{RT}\eta\right)} \right) \quad [50]$$

where

$$X = \frac{i_{0,a}'^2}{i_0'\exp\left(-\frac{\alpha_c F}{RT}\eta\right)} \quad [51]$$

Because the surface coverage of oxygen at all times was assumed to be much smaller than one, the following approximation was made in deriving Eq. 48-51

$$\frac{1-\theta}{1-\theta_0} \approx 1 \quad [52]$$

In Eq. 50 and 51, η is given by Eq. 44, $i_{0,a}'$ is given by Eq. 42, and i_0' is given by Eq. 45.

Thus we have an expression relating the current density (i) to the cell potential (V) in terms of the equilibrium surface coverage (θ_0) and the concentration of oxygen at the surface of the electrode ($c_{O_2,0}$). To complete the derivation, the Langmuir's isotherm for chemisorption is introduced to relate the equilibrium surface coverage to the concentration of the adsorbed species[26,29,30]

$$\theta_0 = \frac{c_{O_2,0}\exp\left(-\frac{\Delta G^0}{RT}\right)}{1 + c_{O_2,0}\exp\left(-\frac{\Delta G^0}{RT}\right)} \quad [53]$$

where ΔG^0 is the Gibbs free energy change for the adsorption process. Because we have assumed that $\theta \ll 1$ under all conditions, this implies that the surface adsorption is not energetically favorable or in other words, the ΔG^0 value for this reaction is a large positive value. Hence, we have

$$\theta_0 \approx c_{O_2,0}\exp\left(-\frac{\Delta G^0}{RT}\right) \quad [54]$$

Equations 42 and 45 are used to calculate $i_{0,a}'$ and $i_{0,1}'$, containing terms that are dependent on the concentration at the surface of the electrode. It is convenient to define these quantities in terms of the exchange current densities defined at reference conditions

$$i_{a,ref} = kc_{O_2,ref} \quad [55]$$

$$i_{0,ref} = k_a'^{\alpha_c/4}k_c^{\alpha_a/4}c_{H^+,ref}^{\alpha_a}(1-\theta_{0,ref})^{\alpha_c/4}\theta_{0,ref}^{\alpha_a/2} \quad [56]$$

Here, $\theta_{0,ref}$ is the fractional coverage of oxygen with respect to a reference solution, which is practically chosen to be 0.5 M H_2SO_4 solution saturated with oxygen. Because the exponent in Eq. 54 is constant at a given temperature, we have

$$\frac{\theta_0}{\theta_{0,ref}} \approx \frac{c_0}{c_{0,ref}} \quad [57]$$

Therefore, Eq. 42 and 45 become

$$i_{0,a}' = i_{a,ref}\frac{c_{O_2,0}}{c_{O_2,ref}} \quad [58]$$

$$i_0' = i_{0,ref}\left(\frac{c_{H^+}}{c_{H^+,ref}}\right)^{\alpha_a}\left(\frac{c_{O_2,0}}{c_{O_2,ref}}\right)^{\alpha_a/2} \quad [59]$$

Once again, in obtaining Eq. 59, the approximation shown in Eq. 52 is used. Note that this approximation assumes that the surface coverage of oxygen is negligible, independent of the potential at the electrode surface. This is not strictly valid at all values of the surface potential. A more rigorous derivation can be obtained using the equations shown in the Appendix. However, closed-form solutions similar to those presented in Eq. 49, 50, and 59 may not be possible. A detailed comparison of the limiting case solution to the rigorous solution will be published elsewhere.

The expression for overpotential in terms of the reference concentrations is given by the following equation[20,22,25]

$$\eta = (\Phi_{met} - \Phi_{RE}) - (\Phi_0 - \Phi_{RE}) - U_{ref} + \frac{RT}{nF}\ln\left(\left(\frac{c_{O_2,0}}{c_{O_2,ref}}\right)^{\alpha_a/2}\left(\frac{c_{H^+,0}}{c_{H^+,ref}}\right)^{\alpha_a}\right) \quad [60]$$

Substituting Eq. 27 into Eq. 60 we have

$$\eta = V - U_{ref} + \frac{RT}{nF}\ln\left(\left(\frac{c_{O_2,0}}{c_{O_2,ref}}\right)^{\alpha_a/2}\left(\frac{c_{H^+,0}}{c_{H^+,ref}}\right)^{\alpha_a}\right) \quad [61]$$

where U_{ref} is defined by Eq. 13.

Thus, the final expression relating the current density (i) to the cell voltage (V) is given by

$$i = i_{a,ref}\frac{c_{O_2,0}}{c_{O_2,ref}}\left(\frac{-X_{ref} + \sqrt{X_{ref}^2 + 4\exp\left(-\frac{\alpha_c F}{RT}\eta\right)\left(X_{ref} + \exp\left(\frac{\alpha_a F}{RT}\eta\right)\right)}}{2\exp\left(-\frac{\alpha_c F}{RT}\eta\right)} - 1 \right) \quad [62]$$

$$X_{ref} = \frac{i_{a,ref}\frac{c_{O_2,0}}{c_{O_2,ref}}}{i_{0,ref}\left(\frac{c_{H^+}}{c_{H^+,ref}}\right)^{\alpha_a}\left(\frac{c_{O_2,0}}{c_{O_2,ref}}\right)^{\alpha_a/2}} \quad [63]$$

Equations 62 and 63 are more convenient to use because the exchange current densities and the overpotential are evaluated at the reference concentrations as opposed to the surface concentrations.

Table II. Parameter values for simulating the polarization curves for the ORR.

Parameters	Reaction 1	Reaction 5	
α_c	0.5–1.5	0.5–1.5	
$i_{0,\mathrm{ref}}$ (A/cm^2)	1×10^{-6}–1×10^{-14}	1×10^{-6}–1×10^{-14}	
U^{θ} (V)	1.229	1.229	
n	4	4	
Solution properties	O_2	H^+	HSO_4^-
$c_{i,\mathrm{ref}}$ (mol/cm^3)	1.13×10^{-6}	5×10^{-4} or 5×10^{-5}	5×10^{-4} or 5×10^{-5}
D_i (cm^2/s)[37,38]	1.79×10^{-5}	9.312×10^{-5}	1.33×10^{-5}
F = 96,487 C/mol	T = 298.15 K	ρ_0 = 0.001 kg/cm^3	Ω = 900 rpm
R = 8.314 J/K mol	U_{re} = 0 V	ν = 0.01187 cm^2/s	$D_R = D_{O_2}$
Reaction properties	O_2	H^+	HSO_4^-
s_i	−1	−4	0
z_i	0	+1	−1
$p_{i,1}$	0	0	
$q_{i,1}$	1	4	
$\gamma_{i,1}$	$1 - \alpha_c/4$	$4 - \alpha_c$	0

Consequently, the exchange current density values can be obtained experimentally at a particular reference condition and the values at other conditions can be calculated readily using Eq. 58 and 59. The exchange current density of the adsorption step $i'_{0,a}$, is linearly proportional to the concentration of oxygen adjacent to the surface of the electrode $c_{O_2,0}$.

Results and Discussion

The governing equations (Eq. 6 and 7) subject to the given boundary conditions (Eq. 8 and 9) are solved numerically by an iterative procedure using both Fortran and Comsol Multiphysics as previously mentioned. The applied potential ($E_{\mathrm{pple}} = \Phi_{\mathrm{met}} - \Phi_{\mathrm{RE}}$) is varied in the range of 1.0–0.0 V and the distribution of c_i and Φ in the electrolyte solution, and the current density i at each specified applied potential E_{pple} are obtained. The plots of i vs E_{pple} are the polarization curves. The parameters used to simulate the ORR in a 0.5 M H_2SO_4 solution at 25°C are shown in Table II. Diffusion coefficients for all species in dilute water were used because literature values for this acidic solution are not readily available.

Parameter estimation and comparison of models.— The utility of the limiting case analysis is significant in obtaining the kinetic parameters from experimental data. No quantitative result distinguishing the surface coverage of individual species on an electrode surface involving multiple reactions is reported in the literature. Hence, we used the limiting case results to obtain the parameters from experimental data using both models for reaction mechanisms 1, 4, and 5 in this work. For the regression scheme, the Gauss–Newton nonlinear parameter estimation method is employed.[31,32] The exchange current density for the charge-transfer step ($i_{0,\mathrm{ref}}$), the cathodic transfer coefficient (α_c), and the diffusion coefficient of oxygen (D_{O_2}) in the electrolyte are regressed simultaneously and the 95% confidence intervals are also calculated.[31] The parameter $i_{a,\mathrm{ref}}$ is assigned a value of 10 A/cm^2, which is a relatively large value so that the adsorption process is fast enough so as not to affect the limiting current densities. One set of regression results with the data digitized from a polarization curve published by Paulus et al.[3] is shown in Fig. 1. The regressed parameter values, 95% confidence

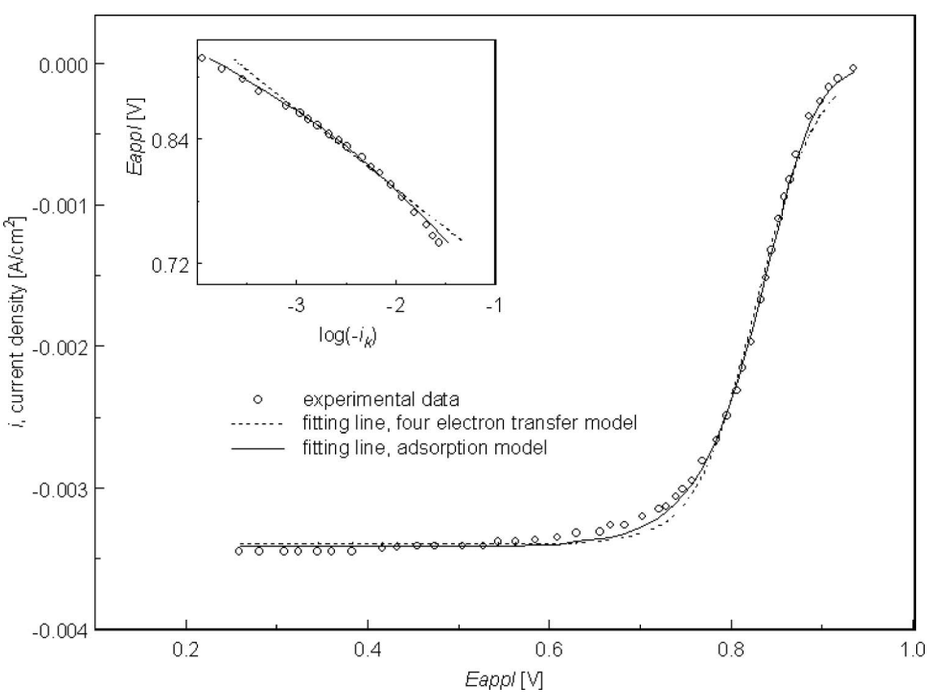

Figure 1. Model predictions compared to the experimental data digitized from Fig. 4 in the paper by Paulus et al.[3] Parameters used to plot: $i_{a,\mathrm{ref}} = 1 \times 10^1$ A/cm^2 for the adsorption model. See Ref. 3 for the operating conditions. See Table III for the regression results.

Table III. Regression results with 95% confidence intervals for the parameter values.

		Four electron-transfer model	Adsorption model
Glassy carbon coated with Pt/C[3] (See Fig. 1 for illustration)	i_0 A/cm^2	$(1.21 \pm 0.22) \times 10^{-7}$	$(2.06 \pm 0.18) \times 10^{-9}$
	α_c	0.776 ± 0.010	1.1427 ± 0.0079
	D_{O_2} cm^2/s	$(1.5410 \pm 0.0030) \times 10^{-5}$	$(1.5537 \pm 0.0018) \times 10^{-5}$
	MSE[a]	7.631×10^{-5}	3.941×10^{-5}
Pt(100)[7]	i_0 A/cm^2	$(8.28 \pm 0.049) \times 10^{-6}$	$(8.89 \pm 0.045) \times 10^{-7}$
	α_c	0.5439 ± 0.0051	0.8074 ± 0.0045
	D_{O_2} cm^2/s	$(2.0945 \pm 0.0039) \times 10^{-5}$	$(2.0379 \pm 0.0023) \times 10^{-5}$
	MSE	6.850e − 5	3.996×10^{-5}
Our data,[b] bare platinum electrode	i_0 A/cm^2	$(3.75 \pm 0.17) \times 10^{-8}$	$(6.397 \pm 0.12) \times 10^{-10}$
	α_c	0.3333 ± 0.0085	0.4741 ± 0.067
	D_{O_2} cm^2/s	$(1.5385 \pm 0.0065) \times 10^{-5}$	$(1.5803 \pm 0.066) \times 10^{-5}$
	MSE	1.197×10^{-4}	1.007×10^{-5}
Our data,[c] glassy carbon coated with Pt/C	i_0 A/cm^2	$(2.10 \pm 0.34) \times 10^{-8}$	$(2.68 \pm 0.23) \times 10^{-10}$
	α_c	0.629 ± 0.055	0.918 ± 0.048
	D_{O_2} cm^2/s	$(0.5528 \pm 0.0068) \times 10^{-5}$	$(0.5543 \pm 0.0051) \times 10^{-5}$
	MSE	3.794×10^{-4}	2.228×10^{-5}

[a] Mean squares of errors.
[b] The data was obtained using a bare Pt RDE (Pine Instruments) at 900 rpm in a 0.5 M H_2SO_4 solution.
[c] The data was obtained using an RDE coated with 30 wt % Pt/C catalyst (provided by E-TEK) at a rotating speed of 900 rpm in a 0.5 M H_2SO_4 solution.

intervals, and the mean square error (MSE), which is calculated as follows[31]

$$MSE = \frac{\sum_{i=1}^{N} (Y_{i,\text{exp}} - Y_{i,\text{pre}})^2}{N - NP} \quad [64]$$

are shown in Table III, along with the results from a few other sets of regressions. Calculation of the residuals based on Eq. 64 ensures that the error is normalized with respect to the degrees of freedom. Note that Paulus et al. obtained their RDE data with a glassy carbon electrode coated with a Pt/C catalyst, and according to the authors, the catalyst layer is thin enough to ignore the mass transfer inside the catalyst layer, so that the ORR mechanism on a smooth planar surface is applicable.

The model with the adsorption mechanism fits the data better visually as seen in Fig. 1, and it is confirmed again by the smaller MSE and the narrower 95% confidence intervals for the regressed parameter values as shown in Table III. The values for the diffusion coefficients D_{O_2} regressed with the two models are about the same, whereas the adsorption model has a significantly smaller value for the exchange current density and a larger transfer coefficient. The same trend is observed in the other three sets of regression results (see Table III). The higher values for the transfer coefficients estimated from the adsorption model indicate that the adsorption process introduces an increase in the resistance to the charge-transfer process, which is counteracted by the increase in the transfer coefficient. In other words, if the ion were to undergo adsorption at the surface of the electrode before the charge-transfer reaction can take place, the gradient in the field that the ion has to traverse across the interface is increased.[33] The validity of the parameters obtained by nonlinear regression is further supported by the calculation of the 95% confidence intervals,[31,32] shown alongside the values of the parameters. The small values for the confidence intervals indicate that the use of the corresponding models is appropriate for the set of data considered.[32]

The comparison of the experimental Tafel slope with those obtained from the two models is shown in the inset of Fig. 1 in the form of Levich–Koutecky plots made with data corrected for mass transfer following the procedure outlined by Bard et al.[7,26,34] As observed, while Reaction 1 predicts a constant slope, the adsorption model shows the change in the Tafel slope similar to the experimental curve. It should be reinforced again that the model equations used in the simulation above assume that the surface coverage is independent of the potential and the influence of the potential dependence of the surface coverage parameter (θ) on the values reported in Table III has not been considered. We did not consider a detailed mechanism[33,35] for the adsorption process either. However, a mechanistic investigation of the adsorption process often results in a more complicated isotherm. Hence, the set of equations describing the new system can readily be obtained by using such an expression in the place of Eq. 53 presented here.

In obtaining Fig. 1 the regressed values for the diffusion and transfer coefficients were used. To compare the adsorption model and the four-electron-transfer model for the same set of parameters, a pair of simulations with both models is shown in Fig. 2. The parameters used are $i_{0,\text{ref}} = 1.0 \times 10^{-8}$ A/cm^2, $\alpha_c = 1.0$, and $D_{O_2} = 1.557 \times 10^{-5}$ cm^2/s for the four-electron-transfer model. In addition to these, $i_{a,\text{ref}} = 10$ A/cm^2 is used for the adsorption model. Note that the value of $i_{a,\text{ref}}$ is relatively big so that the adsorption rate is fast and will not affect the limiting current density. The respective Tafel slopes are shown in the Levich–Koutecky plots inserted in this figure. From this figure, we can see that the model with the adsorption mechanism can predict the change in the Tafel slope. The Tafel slope is roughly doubled in the region where E_{appl} is less than about 0.8 V compared to the region where E_{appl} is higher than about 0.8 V, while the polarization curve corresponding to the four-electron-transfer model has a single Tafel slope until it reaches the limiting current region. The adsorption of oxygen delays the onset of the limiting current density, or in other words, it requires a greater overpotential to reach the limiting current density. The actual value of the voltage at which the slope changes depends on the surface property of the electrodes, electrolyte properties, and the operation conditions.[16]

When the overpotential is small, the reaction rate of the ORR is slow due to the slow charge-transfer step. The adsorption process does not affect the final reaction rate or the polarization curve, because the oxygen concentration next to the surface is relatively high and plenty of oxygen is adsorbed on the surface, whereas only a small amount of the reactant is essential for the ORR to proceed. As the overpotential gets larger, the electrochemical reaction rate gets faster with a greater extent of oxygen consumption, and the oxygen concentration just adjacent to the surface of the electrode is lowered so as to provide a further concentration gradient with respect to the bulk solution so that oxygen can be supplied faster. The rate of

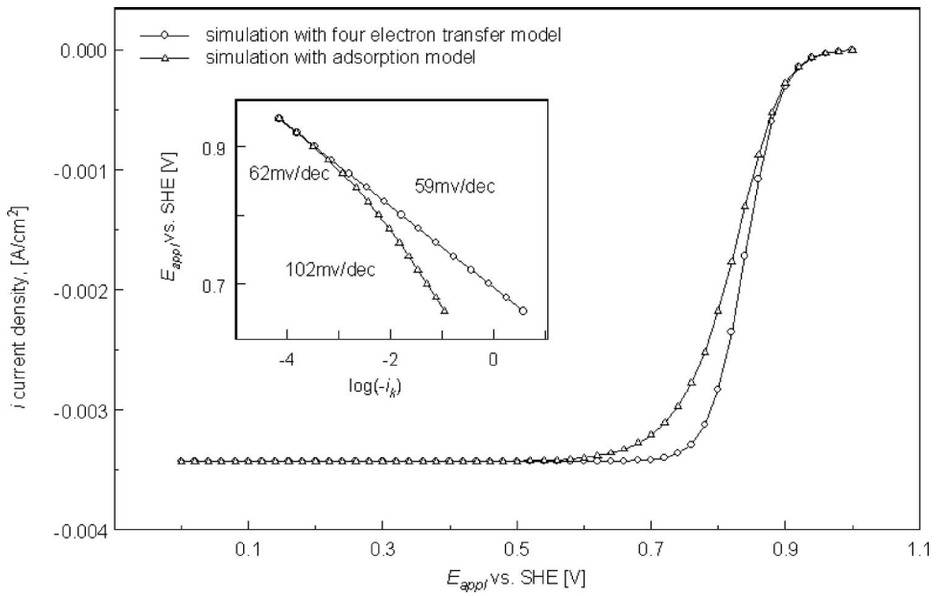

Figure 2. Polarization curves simulated with models for Reactions 1-5. Parameters used to plot: $i_{0,ref} = 1 \times 10^{-8}$ A/cm^2, $\alpha_c = 1.0$, $D_{O_2} = 1.557 \times 10^{-5}$ cm^2/s for the four-electron-transfer model, $i_{a,ref} = 1 \times 10^{1}$ A/cm^2 for the model with the adsorption term.

electrochemical reaction accelerates exponentially as the E_{appl} is decreased linearly, but the adsorption process slows down quickly with the decrease of the oxygen concentration adjacent to the surface of the electrode. Thus, the overall reaction rate is controlled by adsorption once the reaction proceeds into the so-called ohmic region where the polarization curves descend quickly. With the decrease in the applied potential, the overall reaction rate is limited by the supply of oxygen instead of the charge-transfer reaction. Limitation in the supply of oxygen may arise from either the adsorption process being slow or from mass-transfer effects. Figure 2 shows the case that oxygen supply is limited by mass transport because the adsorption process is relatively fast with the assigned value $i_{a,ref} = 10$ A/cm^2. For this case, the apparent limiting current density is the same as that predicted by the four-electron-transfer model or the Levich equation. The case of relatively slower adsorption rate (i.e., with smaller values of $i_{a,ref}$) which can change the limiting current density is discussed in the next section.

Studies of the effect of parameters.— Figure 3 shows the effect of the cathodic transfer coefficient and the exchange current density of the four-electron-transfer model (Reaction 1) on the polarization curves. Again the inserted figure shows the respective Levich–Koutecky plots with mass-transfer-corrected data, while the values of the corresponding Tafel slopes can be found in Table IV. When the transfer coefficient is held constant at 1.0, a change in the exchange current density makes the polarization curve shift horizontally without changing the shape of the curve. But the transfer coefficient affects both the curvature and the position of the curve

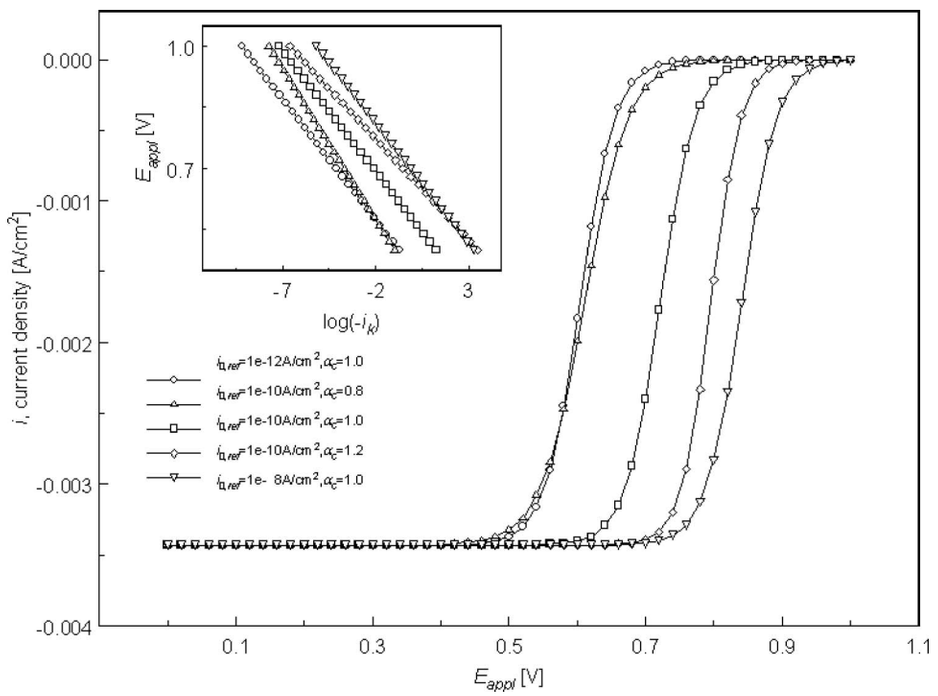

Figure 3. Effect of $i_{0,ref}$ and α_c on polarization curves obtained using the four-electron-transfer model.

Table IV. Apparent Tafel slopes in Fig. 1-6.

	Line description	Voltage at which the slope changes (V)	LCD Tafel slope (mV/dec)		HCD Tafel slope (mV/dec)
In Fig. 1	Experimental data[a]	0.85	58		112
	$i_{0,ref} = 1.21 \times 10^{-7}$ A/cm^2, $\alpha_c = 0.776$[b]	N/A		76	
	$i_{0,ref} = 2.06 \times 10^{-9}$ A/cm^2, $\alpha_c = 1.14$[c]	0.85	58		105
In Fig. 2	$i_{0,ref} = 1 \times 10^{-8}$ A/cm^2, $\alpha_c = 1.0$[b]	N/A		59	
	$i_{0,ref} = 1 \times 10^{-8}$ A/cm^2, $\alpha_c = 1.0$[c]	0.8	62		102
In Fig. 3	$i_{0,ref} = 1 \times 10^{-8}$ A/cm^2, $\alpha_c = 1.0$[b]	N/A		59	
	$i_{0,ref} = 1 \times 10^{-10}$ A/cm^2, $\alpha_c = 0.8$[b]	N/A		74	
	$i_{0,ref} = 1 \times 10^{-10}$ A/cm^2, $\alpha_c = 1.0$[b]	N/A		59	
	$i_{0,ref} = 1 \times 10^{-10}$ A/cm^2, $\alpha_c = 1.2$[b]	N/A		49	
	$i_{0,ref} = 1 \times 10^{-12}$ A/cm^2, $\alpha_c = 1.0$[b]	N/A		59	
In Fig. 4	$i_{0,ref} = 1 \times 10^{-10}$ A/cm^2, $\alpha_c = 1.2$[c]	0.85	56		98
	$i_{0,ref} = 1 \times 10^{-10}$ A/cm^2, $\alpha_c = 1.0$[c]	0.80	62		115
	$i_{0,ref} = 1 \times 10^{-10}$ A/cm^2, $\alpha_c = 0.8$[c]	0.75	76		142
	$i_{0,ref} = 1 \times 10^{-10}$ A/cm^2, $\alpha_c = 0.6$[c]	0.65	101		178
In Fig. 5	$i_{0,ref} = 1 \times 10^{-8}$ A/cm^2, $\alpha_c = 1.0$[c]	0.85	60		109
	$i_{0,ref} = 1 \times 10^{-10}$ A/cm^2, $\alpha_c = 1.0$[c]	0.70	60		110
	$i_{0,ref} = 1 \times 10^{-12}$ A/cm^2, $\alpha_c = 1.0$[c]	0.60	60		113
	$i_{0,ref} = 1 \times 10^{-14}$ A/cm^2, $\alpha_c = 1.0$[c]	0.50	60		110
In Fig. 6	$i_{0,ref} = 1 \times 10^{-8}$ A/cm^2, $\alpha_c = 1.0$[b]	N/A		59	
	Polarization curves with various $i_{a,ref}$[c]	0.80	77		141

[a] Experimental data obtained from Ref. 3.
[b] Simulated results using the four-electron-transfer model.
[c] Simulated results using the adsorption model.

when the exchange current density is held at 1×10^{-10} A/cm^2. Calculated Tafel slopes coincide with the slopes predicted using the Tafel equation given by $2.303RT/(F\alpha_c)$. However, this model predicts only one Tafel slope, and subsequently, the fit to experimental data is not satisfactory.

Figure 4 shows the effect of the transfer coefficient in the adsorption model. The inset figure shows the Levich–Koutecky plots. Table IV contains the respective values of the Tafel slopes. For this case, the transfer coefficient shows about the same effect on the polarization curves as in the four-electron-transfer model, but the Tafel slope changes as shown in the Levich–Koutecky plots. When the exchange current density is held at 1×10^{-10} A/cm^2, the Tafel slope changes at higher potentials for the cases where the transfer coefficient is larger. The Tafel slopes at the LCD region coincide with the predictions from the Tafel equation, while the Tafel slopes in the HCD region are roughly doubled compared to the slopes in the LCD region.

Figure 5 and the data in Table IV show the effect of the exchange current density in the adsorption model. The turning points of the Tafel plots are at higher potentials as the exchange current densities become larger, when the transfer coefficient is held constant at a

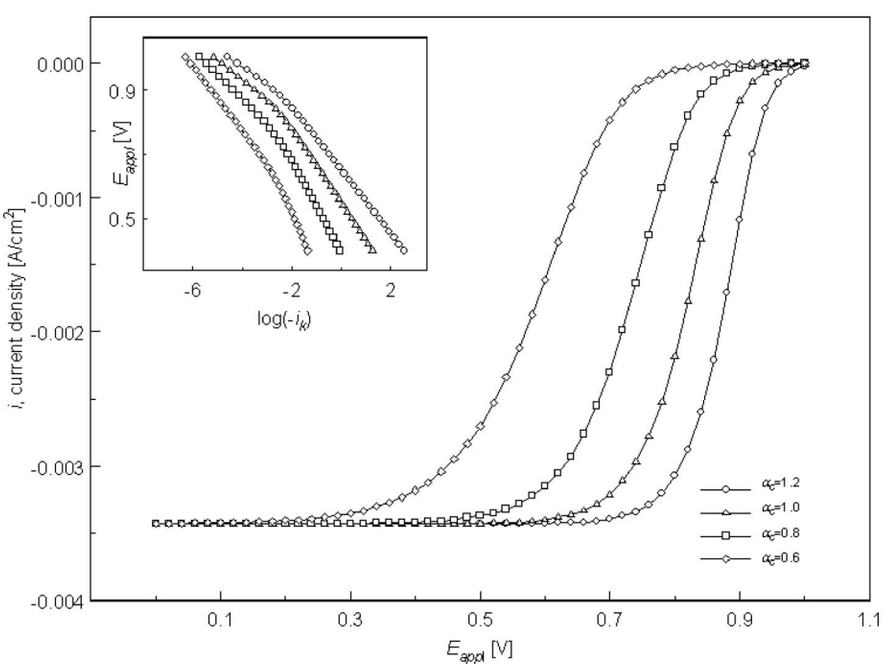

Figure 4. Effect of α_c in the adsorption model. Parameters used in the plot: $i_{0,ref} = 1 \times 10^{-8}$ A/cm^2, $D_{O_2} = 1.557 \times 10^{-5}$ cm^2/s, and $i_{a,ref} = 1 \times 10^{1}$ A/cm^2.

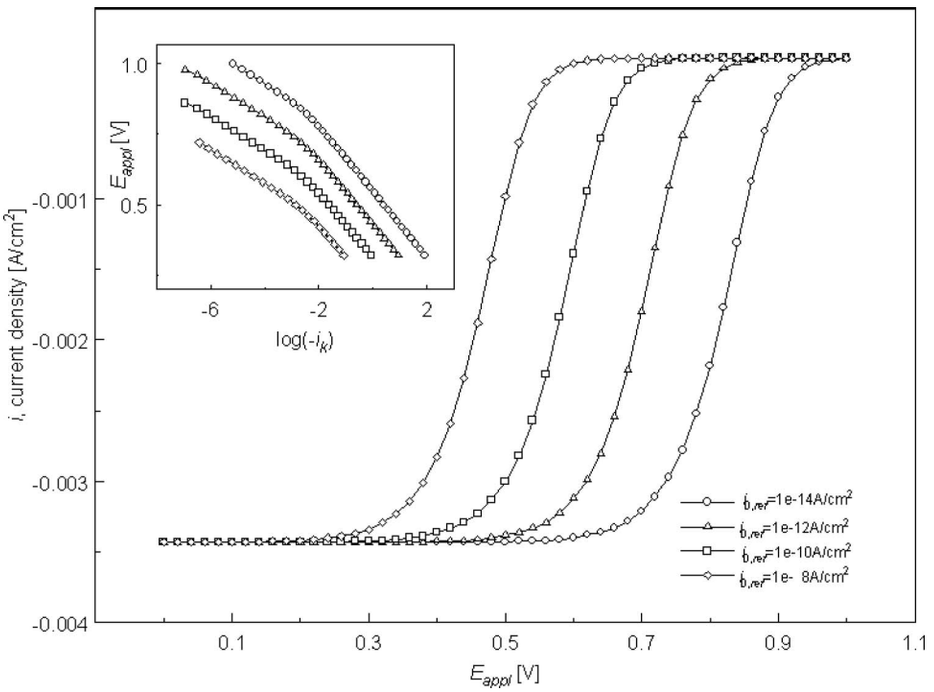

Figure 5. Effect of $i_{0,\mathrm{ref}}$ in the adsorption model. Parameters used in the plot: $\alpha_c = 1.0$, $D_{O_2} = 1.557 \times 10^{-5}$ cm^2/s, and $i_{a,\mathrm{ref}} = 1 \times 10^{1}$ A/cm^2.

certain value, 1.0 in this case. But the Tafel slopes do not change significantly, as shown in Table IV. The LCD Tafel slopes follow the prediction of the Tafel equation for this case also.

The only adsorption-related parameter which has an effect on the polarization curves is the exchange current density $i_{a,\mathrm{ref}}$ according to Eq. 62 and 63. Figure 6 shows a set of polarization curves with different values for $i_{a,\mathrm{ref}}$, and Fig. 7 is a plot of $i_{a,\mathrm{ref}}$ vs the limiting current densities. The adsorption affects the apparent limiting current density only if the value of $i_{a,\mathrm{ref}}$ is less than a critical value, which is about 1 A/cm^2 in this calculation. The adsorption process limits the overall reaction rate before the mass-transfer limit is reached, and the apparent limiting current density does not follow the Levich equation for this case. Figure 7 shows how the parameter $i_{a,\mathrm{ref}}$ affects the limiting current density and reinstates the observations made above. The Tafel slopes do not change with the rate of adsorption, as shown in the inset in Fig. 6.

Conclusion

An adsorption model for the ORR at an RDE was developed based on the oxygen adsorption mechanism. The conventional four-electron-transfer model was also simulated for comparison. The fit to experimental data using both these models was carried out by

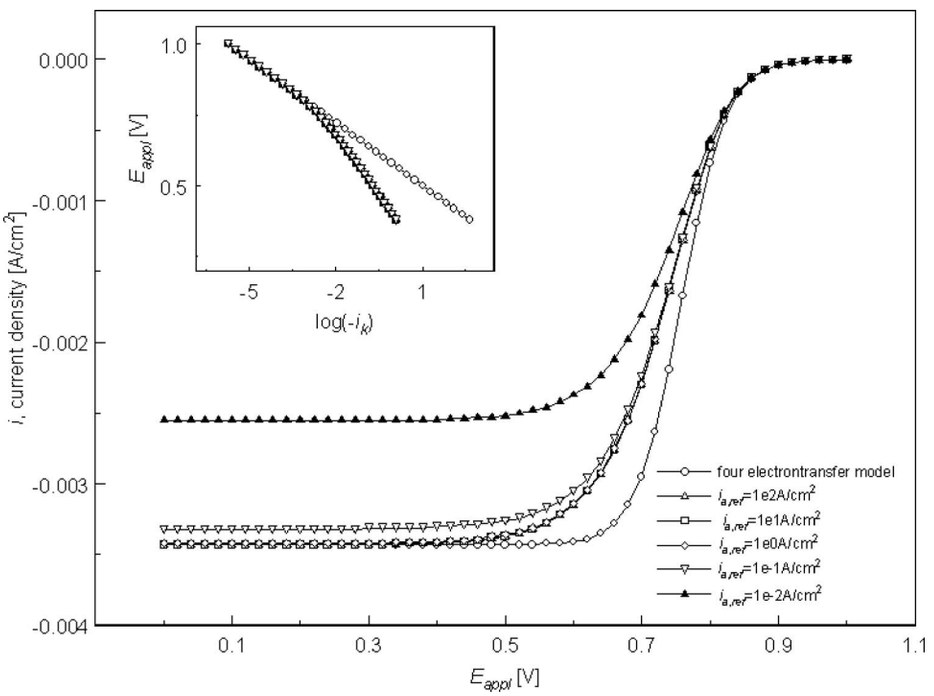

Figure 6. Effect of $i_{a,\mathrm{ref}}$ in the adsorption model. Parameters used in the plot: $i_{0,\mathrm{ref}} = 1 \times 10^{-8}$ A/cm^2, $\alpha_c = 1.0$, and $D_{O_2} = 1.557 \times 10^{-5}$ cm^2/s.

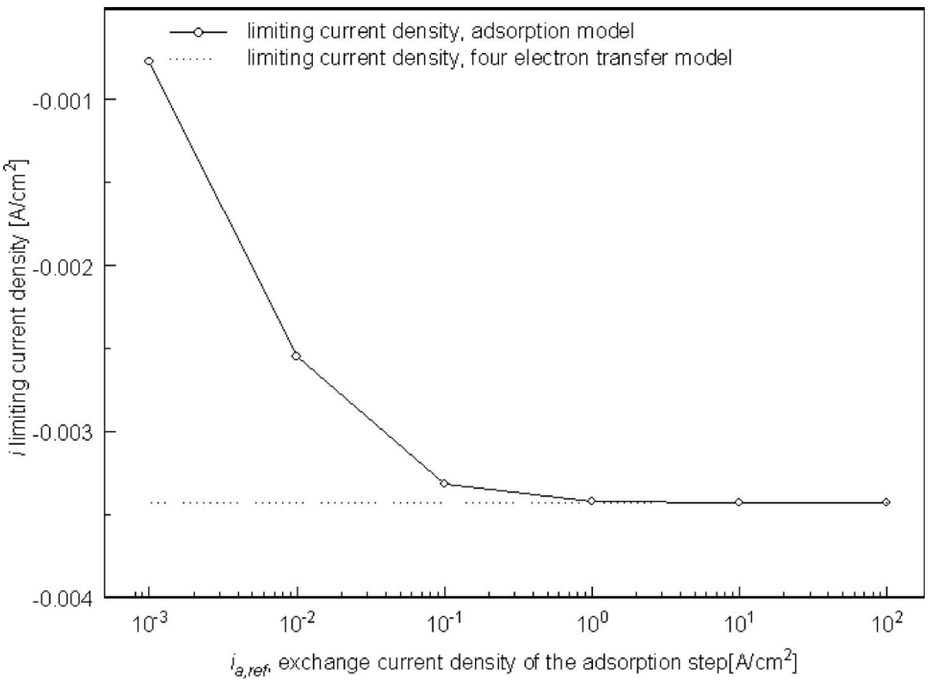

Figure 7. Effects of $i_{a,ref}$ on the limiting current density. Parameters in the plot: $i_{0,ref} = 1 \times 10^{-8}$ A/cm^2, $\alpha_c = 1.0$, $D_{O_2} = 1.557 \times 10^{-5}$ cm^2/s.

nonlinear parameter estimation for a limiting case, and the results indicate that the adsorption model fits the experimental data better. The study of the effect of the kinetic parameters in both models shows that the adsorption model can predict the double Tafel slope phenomenon. The existence of a critical adsorption rate below which the adsorption process limits the overall reaction rate is observed.

Acknowledgments

The authors are grateful for the financial support provided by the U.S. Department of Energy under cooperative agreement no. DE-FC36-04GO14232.

The University of South Carolina assisted in meeting the publication costs of this article.

Appendix

From Eq. 40 and 41 above, we have

$$i_a = i'_{0,a}\frac{\theta - \theta_0}{\theta_0} \quad [A\text{-}1]$$

$$i = i'_0\left[\frac{1-\theta}{1-\theta_0}A - \left(\frac{\theta}{\theta_0}\right)^2 B\right] \quad [A\text{-}2]$$

where

$$A = \exp\left(\frac{\alpha_a F}{RT}\eta\right) \quad [A\text{-}3]$$

$$B = \exp\left(-\frac{\alpha_c F}{RT}\eta\right) \quad [A\text{-}4]$$

Solving Eq. A-2 through A-4 for θ we have

$$\theta = \frac{\theta_0}{2i'_0 B(\theta_0 - 1)}[Ai'_0\theta_0 - \sqrt{A^2 i'^2_0\theta_0^2 - 4ii'_0 B + 8ii'_0 B\theta_0 + 4i'^2_0 AB - 4Bii'_0\theta_0^2 - 4ABi'^2_0\theta_0}] \quad [A\text{-}5]$$

Substituting the expression for θ in A-1 and solving for i we have

$$i = \frac{1}{2}\left[2Bi'_0 - 2Bi'_0\theta_0 + i'_{0,a} + Ai'_0\theta_0 - \theta_0 i'_{0,a} - \frac{i'_{0,a}}{i'_0 B(\theta_0 - 1)}\sqrt{4Bi'_{0,a}i'_0 + 4Bi'_0 i'_{0,a}\theta_0^2 - 2Ai'_0 i'_{0,a}\theta_0^2 + A^2 i'^2_0\theta_0^2 - 4ABi'^2_0\theta_0 + 2Ai'_{0,a}i'_0\theta_0 - 8Bi_a i'_0\theta_0 + i'^2_{0,a} + \theta_0^2 i'^2_{0,a} - 2\theta_0 i'^2_{0,a} + 4ABi'^2_0}\right] \quad [A\text{-}6]$$

Equations A-6 and 61 can now be used to relate the current and potential in terms of the concentration of oxygen at the surface and the equilibrium surface coverage. The equilibrium coverage can be obtained from Eq. 53 or other expressions for the isotherm, which involve interaction parameters to account for the presence of other species and/or the dependence on potential.[36] However, note that these equations have to be solved numerically now, because a closed-form solution does not exist for this case.

List of Symbols

c_i	concentration of species i, mol/cm^3
$c_{i,RE}$	concentration of species i at reference electrode, mol/cm^3
$c_{i,ref}$	concentration of species i at reference concentrations, mol/cm^3
$c_{i,0}$	concentration of species i at equilibrium with the solution adjacent to the surface of electrode, in Reactions 2-5, mol/cm^3
$c_{i,\infty}$	concentration of species i in the bulk solution, mol/cm^3
$c_{R_l,ads}$	transient concentration of species l adsorbed on the electrode surface, mol/cm^3
D_i	diffusion coefficient of species i, cm^2/s
D_R	diffusion coefficient of the limit reactant, cm^2/s
E_{appl}	applied potential between working electrode and reference electrode, V
F	Faraday's constant, 96,487 C/mol
ΔG^0	free energy change for adsorption process, J/mol
i	current density across the cell, A/cm^2
$i_{a,l}$	current density of adsorption step of process l as Reaction 2, A/cm^2
i_j	current density of reaction j, A/cm^2
$i_{0,j}$	exchange current density of the reaction j at concentrations adjacent to the electrode surface, A/cm^2
$i_{0,j,ref}$	exchange current density of the charge transfer reaction j at reference concentrations, A/cm^2

$i'_{0,a,l}$ exchange current density of the adsorption step l in Reactions 2-5 corresponding to concentrations adjacent to electrode surface, A/cm^2
$k_{l,ads}$ proportionality constant between $c_{R_j,ads}$ and θ_l for adsorption Reaction 1
$k''_{a,j}$, $k'_{c,j}$ potential-independent rate constants for anodic and cathodic directions of charge-transfer step in Reaction 3, units vary
$k'_{a,j}$, $k_{c,j}$ potential-independent rate constants combined with the constant concentrations for anodic and cathodic directions of the charge-transfer step, units vary
k_l, k''_l potential-independent rate constants for the adsorption step of the adsorption process l, A/cm^2
$M_{i,j}$ reaction species i in reaction j
N number of experimental data points
NP number of the parameters regressed
n_j number of electrons transferred in reaction j
$n_{j,RE}$ number of electrons transferred in the reaction that occurs at the reference electrode
n_s total number of the adsorption process
$O_{2,ads}$ O_2 absorbed at the surface of the electrode
$O_{2,sur}$ O_2 in the solution phase adjacent to the surface of the electrode
$p_{i,j}$ anodic reaction order of species i in the reaction j
R universal gas constant, 8.3143 J/mol K
P_i species i which does not undergo adsorption and can involve a charge-transfer reaction on the electrode surface directly
$q_{i,j}$ cathodic reaction order of species i in the reaction j
$R_{l,sur}$ species l in the solution phase adjacent to the electrode surface
$R_{l,ads}$ species l adsorbed on the electrode surface
$s_{i,j}$ stoichiometric coefficient of species i or l in reaction j
$s_{i,j,RE}$ stoichiometric coefficient of species i in reaction j at reference electrode
T absolute temperature, K
U^θ_j standard electrode potential for the charge-transfer reaction j, V
$U^\theta_{j,RE}$ potential of the standard reference electrode relative to SHE, V
$U_{ref,j}$ open-circuit potential of the reaction j at the reference concentrations relative to a standard reference electrode of a given kind, V
V potential of the working electrode, V
$V'_{0,j}$ potential of the working electrode with respect to reaction mechanism 3 while the working electrode is in equilibrium with a solution of composition the same as that immediately adjacent to the surface of the working electrode, V
X a grouping variable as defined in Eq. 51
X_{ref} defined at the reference conditions (see Eq. 63)
$Y_{i,exp}$ ith experimental data
$Y_{i,pre}$ model prediction of the ith data point
y distance from electrode surface into the electrolyte, cm
z_i charge on species i

Greek

$\alpha_{a,j}$, $\alpha_{c,j}$ anodic and cathodic transfer coefficient for the charge-transfer reaction j
$\gamma_{i,j}$ exponent in the composition dependence of the exchange current density
δ_D diffusion layer thickness, $\delta_D = (3D_R/0.51032\nu)^{1/3}(\nu/\Omega)^{1/2}$, cm
η_j overpotential of reaction j corrected for ohmic drop in the solution measured with respect to the reference electrode of a given kind containing a solution at the reference concentrations, V
θ fractional coverage of the electrode surface by oxygen
θ_0 equilibrium fractional surface coverage of oxygen with respect to the concentration of the solution adjacent to the electrode surface
$\theta_{l,0}$ equilibrium fractional surface coverage of species l with respect to the concentration of the solution adjacent to the electrode surface
$\theta_{0,ref}$ relative surface coverage of oxygen respect to reference concentration at equilibrium
ν kinematic viscosity, cm^2/s
ξ dimensionless distance from electrode surface into electrolyte, y/δ_D
ρ_0 density of the pure solvent, kg/cm^3
Φ potential in the solution within the diffusion layer, V
Φ_0 potential in the solution adjacent to the electrode surface, V
Φ_{RE} potential of the reference electrode at the experimental conditions, V
Φ_{met} potential of working electrode, V
Ω rotating speed of electrode, rad/s

References

1. T. J. Schmidt, U. A. Paulus, H. A. Gasteiger, and R. J. Behm, *J. Electroanal. Chem.*, **508**, 41 (2001).
2. V. Stamenkovic, T. J. Schmidt, P. N. Ross, and N. M. Markovic, *J. Phys. Chem. B*, **106**, 11970 (2002).
3. U. A. Paulus, T. J. Schmidt, H. A. Gasteiger, and R. J. Behm, *J. Electroanal. Chem.*, **495**, 134 (2001).
4. V. Srinivasamurthi, R. C. Urian, and S. Mukerjee, in *Proton Conductivity Membrane Fuel Cells III*, M. Murthy, T. F. Fuller, J. W. Van Zee, and S. Gottesfeld, Editors, PV 2002–31, p. 99, The Electrochemical Society Proceedings Series, Pennington, NJ (2002).
5. M. R. Tarasevich, A. Sadkowski, and E. Yeager, *Comprehensive Treatise of Electrochemistry*, Vol., 7, *Kinetics and Mechanisms of Electrode Processes*, P. Horsman, B. E. Conway, and E. Yeager, Editors, p. 354, Plenum Press, New York (1983).
6. P. S. D. Brito and C. A. C. Sequeira, *J. Power Sources*, **52**, 1 (1994).
7. N. M. Markovic, H. A. Gasteiger, and P. N. Ross, Jr., *J. Phys. Chem.*, **99**, 3411 (1995).
8. C. F. Zinola, A. M. C. Luna, W. E. Triaca, and A. J. Arvia, *Electrochim. Acta*, **39**, 1627 (1994).
9. B. N. Grgur, N. M. Markovic, and P. N. Ross, *Can. J. Chem.*, **75**, 1465 (1997).
10. A. Parthasarathy, S. Srinivasan, A. J. Appleby, and C. R. Martin, *J. Electrochem. Soc.*, **139**, 2530 (1992).
11. U. A. Paulus, A. Wokaun, G. G. Scherer, T. J. Schmidt, V. Stamenkovic, N. M. Markovid, and P. N. Ross, *Electrochim. Acta*, **47**, 3787 (2002).
12. A. Damjanovic and M. A. Genshaw, *Electrochim. Acta*, **15**, 1281 (1970).
13. A. Damjanovic and V. Brusic, *Electrochim. Acta*, **12**, 615 (1967).
14. A. Parthasarathy, C. R. Martin, and S. Srinivasan, *J. Electrochem. Soc.*, **138**, 916 (1991).
15. A. K. N. Reddy, M. Genshaw, and J. O'M. Bockris, *J. Electroanal. Chem.*, **8**, 406 (1964).
16. M. M. Markovic, R. R. Adzic, B. D. Cahan, and E. B. Yeager, *J. Electrochem. Soc.*, **377**, 249 (1994).
17. P. E. Kadiri, F. Faure, and R. Durand, *J. Electroanal. Chem. Interfacial Electrochem.*, **301**, 177 (1991).
18. R. Woods, *Electroanalytical Chemistry*, Vol. 9, *Chemisorption at Electrodes: Hydrogen and Oxygen on Noble Metals and Their Alloys*, A. J. Bard, Editor, p. 59, Marcel Dekker, Inc., New York (1976).
19. G. Tamizhmani, J. P. Dodelet, and D. Guay, *J. Electrochem. Soc.*, **143**, 18 (1996).
20. R. E. White, S. E. Lorimer, and R. Darby, *J. Electrochem. Soc.*, **130**, 1123 (1983).
21. R. E. White and S. E. Lorimer, *J. Electrochem. Soc.*, **130**, 1096 (1983).
22. P. K. Adanuvor, R. E. White, and S. E. Lorimer, *J. Electrochem. Soc.*, **134**, 625 (1987).
23. R. Darby, *Advanced Energy Conversion*, **5**, 43 (1965).
24. R. E. White, M. A. Nicholson, L. G. Kleine, J. V. Zee, and R. Darby, *J. Electrochem. Soc.*, **131**, 268 (1984).
25. P. K. Adanuvor and R. E. White, *J. Electrochem. Soc.*, **134**, 1093 (1987).
26. A. J. Bard and L. R. Faulkner, *Electrochemical Methods*, 2nd ed., John Wiley & Sons, New York (2004).
27. R. Woods, in *Electroanalytical Chemistry*, Vol. 9, A. J. Bard, Editor, Marcel Decker Inc., New York (1976).
28. B. E. Conway and S. Gottesfeld, *J. Chem. Soc., Faraday Trans. 1*, **69**, 1090 (1973).
29. S. Lowell, *Introduction to Powder Surface Area*, John Wiley & Sons, New York (1979).
30. S. E. Lorimer, M.Sc. Thesis, Department of Chemical Engineering, Texas A&M University, College Station, TX (1982).
31. A. Constantinides and N. Mostoufi, *Numerical Methods for Chemical Engineers with Matlab Applications*, Prentice Hall PTR, Englewood Cliffs, NJ (1999).
32. Y. Bard, *Nonlinear Parameter Estimation*, Academic Press, Inc., New York (1974).
33. A. B. Anderson and T. V. Albu, *J. Electrochem. Soc.*, **147**, 4229 (2000).
34. T. J. Schmidt, H. A. Gasteiger, G. D. Stab, P. M. Kolb, and R. J. Behm, *J. Electrochem. Soc.*, **145**, 2354 (1998).
35. J. K. Nørskov, J. Rossmeisl, A. Logadottir, and L. Lindqvist, *J. Phys. Chem. B*, **108**, 17886 (2004).
36. J. O'M. Bockris, A. K. N. Reddy, and M. G. Aldeco, *Modern Electrochemistry*, Vol. 2A, Kluwer Academic/Plenum Publishers, New York (2000).
37. J. S. Newman and K. E. Thomas-Alyea, *Electrochemical Systems*, 3rd ed., John Wiley & Sons, Inc., New York (2004).
38. M. F. Easton, A. G. Mitchell, and W. F. K. Wynne-Jones, *Trans. Faraday Soc.*, **48**, 796 (1952).